Environ. Eng. Res. 2017; 22(1): 95-107
https://doi.org/10.4491/eer.2016.094

pISSN 1226-1025
eISSN 2005-968X

Adsorption isotherm and kinetics analysis of hexavalent chromium and mercury on mustard oil cake

T. Vishnuvardhan Reddy, Sachin Chauhan, Saswati Chakraborty†

Department of Civil Engineering, Indian Institute of Technology Guwahati, Assam-781039, India

ABSTRACT

Adsorption equilibrium and kinetic behavior of two toxic heavy metals hexavalent chromium [Cr(VI)] and mercury [Hg(II)] on mustard oil cake (MOC) was studied. Isotherm of total chromium was of concave type (S1 type) suggesting cooperative adsorption. Total chromium adsorption followed BET isotherm model. Isotherm of Hg(II) was of L3 type with monolayer followed by multilayer formation due to blockage of pores of MOC at lower concentration of Hg(II). Combined BET-Langmuir and BET-Freundlich models were appropriate to predict Hg(II) adsorption data on MOC. Boyd's model confirmed that external mass transfer was rate limiting step for both total chromium and Hg(II) adsorptions with average diffusivity of 1.09×10^{-16} and 0.97 m^2/sec, respectively. Desorption was more than 60% with Hg(II), but poor with chromium. The optimum pH for adsorptions of total chromium and Hg(II) were 2-3 and 5, respectively. At strong acidic pH, Cr(VI) was adsorbed by ion exchange mechanism and after adsorption reduced to Cr(III) and remained on MOC surface. Hg(II) removal was achieved by complexation of $HgCl_2$ with deprotonated amine ($-NH_2$) and carboxyl (COO-) groups of MOC.

Keywords: BET-Freundlich isotherm, BET-Langmuir isotherm, L3 type isotherm, Pore blockage, S1 type isotherm

1. Introduction

Cr(VI) and Hg(II) are considered as two toxic metals found in the environment. Cr(VI) is discharged from tannery, electroplating, metal plating, petroleum refining activities [1, 2]. Several industries like chlor-alkali, battery manufacturing, mining activities, oil and coal combustion, cement production, from scrubber water of coal fired plant, electronics manufacturing plant etc. are responsible for discharge of mercury in environment [2]. In India the maximum concentrations allowed to discharge in inland surface water are 0.01 mg/L for Hg(II) and 0.1 mg/L for Cr(VI) and 2 mg/L for total chromium [Cr(VI) + Cr(III)] [3].

Adsorption is a highly cost-effective and versatile technology for removal of metal ions from wastewater. In recent years agricultural by products like orange peel, rice husk hazelnut shell, pine bark, etc. were used as biosorbents for removal of several metal ions from wastewater [4, 5]. These agricultural by products are of low cost, biodegradable materials with several functional groups, which act as binding sites for metal ions. A recent review is available on several biosorbents for removal of chromium and Hg(II) from wastewater [6].

Mustard, a common oil plant available in India belongs to *Brassicaceae* family [7]. After oil extraction, the solid residue is known as mustard oil cake (MOC). It is used as nitrogenous manure for crops and animal feed [8]. MOC was used for removal of divalent metals like nickel, cadmium and copper [7-9] and very high removals were achieved with copper ion (454 mg/g) as compared to nickel (3 mg/g) and cadmium (33 mg/g). In aqueous solution, Cr(VI) remains as oxyanion unlike divalent copper, cadmium and nickel and Hg(II) forms strong complexes with chloride ion and removal of Hg(II) from Hg-Cl complexes is difficult.

Most of the published work with MOC and other biosorbents for metal ion removals mainly emphasized on metal uptake value without in-depth analysis of adsorption equilibrium behavior, mechanism of adsorption and mechanistic steps involved in adsorption process. In the present study equilibrium and kinetic behaviors of Cr(VI) and Hg(II) on MOC was studied and mechanism of adsorption of these metal ions by MOC was identified.

Received July 21, 2016 **Accepted** October 31, 2016

† Corresponding author
Email: saswati@iitg.ernet.in
Tel: +91-361-2582412 Fax: +91-361-2690762

2. Materials and Methods

2.1. Materials

Oil was extracted from the mustard seeds and waste matter left after extraction is known as MOC. MOC used in this study as adsorbent was obtained from a small oil mill of Vikasnagar (Uttarakhand, India). MOC was washed with Millipore water in order to remove the oil and impurities. 250 mL of millipore water was used to wash 5 gm of MOC for 4 to 5 times and then kept in oven at 80℃ for 6 h. The dried MOC was stored in a beaker in desiccators and used as adsorbent for this study.

2.2. Adsorption Experiment

Solution pH, dose of adsorbent, initial concentration of metal ions, effect of competitive ions were variable parameters for this study. In order to study the effect of solution pH, studies were carried out both at uncontrolled and controlled condition. At uncontrolled pH condition, initial pH of solution was adjusted from 2 to 10 for Cr(VI) and from 2 to 7 for Hg(II) using 100 mL of 50 mg/L metal solution. Initial solution pH was adjusted using hydrochloric acid (HCl) and sodium hydroxide (NaOH) of 0.01/0.1 N. 2 g/L of MOC was used and solution pH was left uncontrolled during this experiment. The mixing of MOC in metal solution was achieved in a horizontal shaker at 150 rpm for 3 h. Then effect of controlled solution pH was carried out in a similar way using acetate buffer (of 0.1 mM/L) of required volume to maintain the pH constant during the experiment.

Dose of MOC was varied from 0.1 to 15 g/L with initial concentration of metal ion of 50 mg/L. For Cr(VI), initial solution pH was 2 and 3 and left uncontrolled and for Hg(II) solution pH was constant at 4 and 5 and study was done for 24 h. Initial concentration of Cr(VI) and Hg(II) was varied from 10 to 100 mg/L with 100 mL metal solution in several plastic sealed bottles. MOC added bottles were kept in horizontal shaker at 30℃ temperature at 150 rpm. At regular time interval each plastic bottle was withdrawn from shaker.

Effect of other ions on removal of chromium and Hg(II) was studied in presence of common anions present in water like nitrate (NO_3^-), sulphate (SO_4^{2-}), and phosphate (PO_4^{3-}). The respective salts used were: KNO_3, Na_2SO_4, and KH_2PO_4. Study was carried out separately with each anion of varying strength (0.01-1 mM/L). Study was carried out with Cr(VI) of 50 mg/L at uncontrolled pH of 2 along with a control (without other ion). In a likely manner study was also carried out with Hg(II) of 50 mg/L at controlled pH of 4.

After adsorption experiment, samples were filtered using Whatman filter paper (grade 1) and final pH and residual total chromium concentration and residual Hg(II) concentrations were estimated. For Cr(VI) adsorption study at varying pH, residual concentration of Cr(VI) was also estimated in filtered samples.

The amount of metal adsorbed on MOC was calculated based on the difference of metal concentrations in aqueous solution before and after adsorption experiment according to Eq. (1).

$$q_t = \frac{(C_0 - C_t) \times V}{m} \quad (1)$$

where, q_t is the amount of metal adsorbed per unit weight of adsorbent (mg/g) at time t, C_0 and C_t are the concentrations of metal (mg/L) at initial time and at time t respectively, V is the initial volume of metal solution (L) and m is the mass of MOC (g). When t is equal to the equilibrium time, $C_t = C_e$, $q_t = q_e$, then the amount of metal adsorbed at equilibrium was calculated using the same Eq. (1).

2.3. Desorption and Reuse Study

Initially, adsorption study was performed separately with 100 mL of Cr(VI) and Hg(II) of concentration 50 mg/L for 12 h at uncontrolled pH of 3 and controlled pH of 4, respectively. Then the adsorbent was collected and dried at 60˚C and dried adsorbent was used for desorption experiment. For total chromium desorption, different concentrations of NaOH (0.1-6 N) and EDTA (0.02-0.2 N) were used as desorbents. Desorbent volume of 50 mL was taken for each case and desorption experiments were performed in a horizontal shaker at 150 RPM for 12 h. Then the samples were filtered and analyzed for final concentration of total chromium and Cr(VI). For Hg(II), desorption experiment was carried out similarly using KI, HCl and NaOH as desorbents. Desorption amount was calculated using Eq. (2).

$$Desorption(\%) = \frac{(V_{des} \times C_{des}) \times 100}{(C_0 - C_e)\, V_{ads}} \quad (2)$$

where, V_{des} is the volume of desorbent used (50 mL), C_{des} is the final concentration of metal in solution after desorption (mg/L), C_e is equilibrium metal concentration after adsorption (mg/L), C_0 is the initial metal concentration before adsorption (mg/L) and V_{ads} is the volume of metal solution used for adsorption experiment (250 mL).

For reuse study, after desorption process with NaOH, MOC was collected and washed with distilled water and then dried in oven and reused for another cycle. This process was repeated for four cycles (each cycle of adsorption-desorption) with fresh metal solution in each cycle.

2.4. Analytical Procedure

Zero point charge of MOC was estimated using immersion technique as described by Fiol and Villaescusa [10]. FESEM and EDX analysis was performed to get image of surface and presence of elements (Hitachi 5500 FESEM). Particle size distribution of MOC was determined using a particle size analyzer (Mastersizer 2000, Malvern). Specific surface area, pore size and pore volume of MOC were determined from BET surface area analysis (Autosorb- IQ MP). Surface groups on MOC were estimated using FTIR technique (Fourier Transfer Infrared Resonance) (Perkin Elmer, PE-RXI).

Concentrations of total chromium in aquatic solutions were evaluated using atomic absorption spectrophotometer (AAS) at specified wavelengths of 428.9 nm (slit width 0.5 nm). Hg(II) con-

centration was estimated using AAS at wavelength of 253.7 nm, silt width 0.5 mm (Spectra AA Varian, 55B). Cr(VI) concentration was estimated using spectrophotometer at wavelength of 540 nm by 1,5- diphenyl carbazide method [11].

3. Results and Discussion

3.1. Characterization of MOC

MOC was observed to contain 4.1% volatile solids and 95.9% fixed solids by weight with density of 1,369 kg/m^3. pH_{zpc} plays an important role in characterizing the nature of the surface of any adsorbent. The graph for the determination of pH_{zpc} of MOC is shown in Fig. 1(a). pH_{zpc} of MOC surface was observed at 5.3. The results of the particle size analysis based on the differential volume, as shown in Fig. 1(b). 10% of the particles in the tested sample were smaller than 317 μm, 50% of the particles were smaller than 657 μm and 90% of the particles were smaller than 1,317 μm.

The surface area of the MOC was determined using standard nitrogen adsorption porosimetric technique employing the BET method. N_2 adsorption isotherm on MOC is shown in Fig. 2(a). Multi-point BET analysis showed that BET specific surface area was 14.84 m^2/g. Pore size distribution of MOC is given in Fig. 2(b).

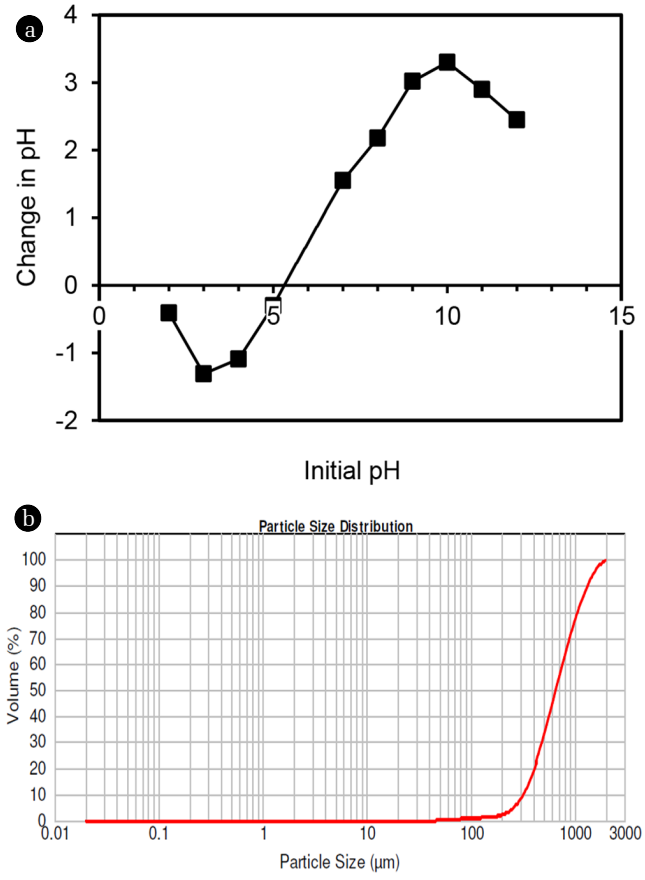

Fig. 1. (a) zero point charge and (b) particle size distribution of MOC.

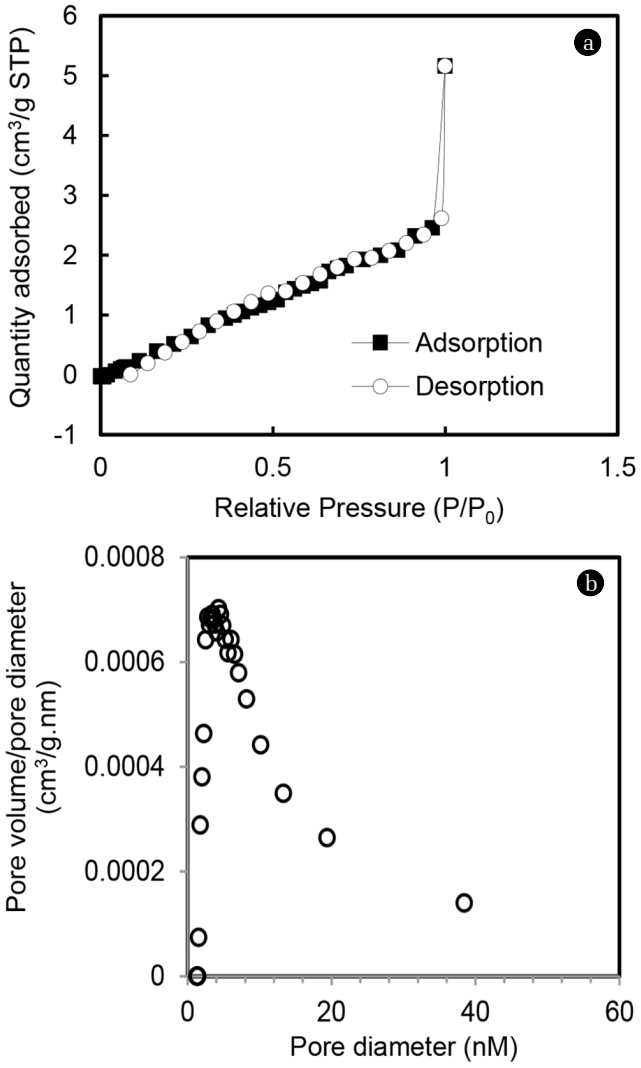

Fig. 2. (a) N_2 adsorption isotherm of MOC and (b) pore size distribution of MOC.

It can be seen that MOC had predominant contribution in the mesopore range (2-50 nm). Pore volume of MOC was determined by employing the BJH method and pore volume was 0.010 cc/g.

The FTIR spectrum of MOC before and after Hg(II) and Cr(VI) adsorption is shown in Fig. 3. The broad absorption peaks between 3,300-3,250 cm^{-1} was due to cellulose, pectin, lignin and absorbed water [5]. The band at 3,000-2,850 cm^{-1} can be assigned to the CH stretching and the peak at 2,362 cm^{-1} was due to NH stretching [7]. The absorption bands at 1,753 cm^{-1} can be attributed to C = O stretch, due to carboxylic acid [12]. The peak at 1,085 cm^{-1} was due to C-N stretching [7, 13]. Significant change in band position was observed after adsorption of metal ions and change was more profound for Cr(VI) than Hg(II). EDX spectra of MOC after Cr(VI) and Hg(II) adsorption are shown in Fig. 4, which proves presence of chromium and mercury ions on MOC surface.

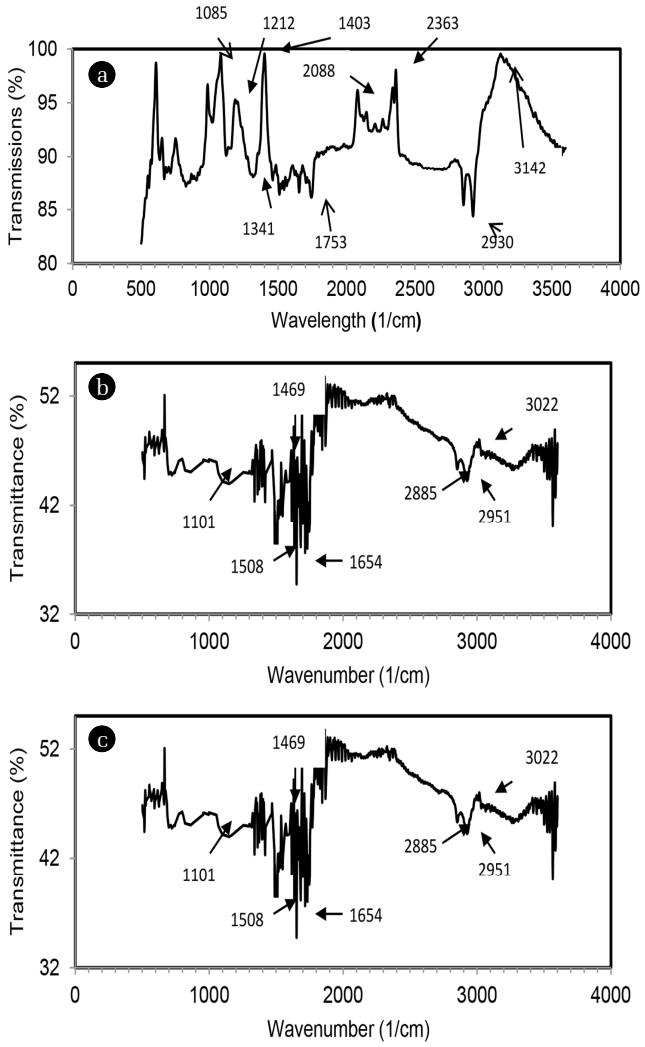

Fig. 3. FTIR spectra of (a) MOC, (b) after Hg(II) adsorption and (c) after Cr(VI) adsorption.

3.2. Effect of Initial Solution pH

Effect of pH on Cr(VI) adsorption was studied both at controlled and uncontrolled condition at varying pH of 2-10. Residual chromium was analyzed as total chromium [Cr(VI) + Cr(III)] and Cr(VI). Concentration of Cr(III) was calculated form the difference of total chromium and Cr(VI). Results of pH effect are shown in Fig. 5(a)-(d).

Acidic pH favoured total chromium adsorption and removal decreased with increasing pH for both controlled and uncontrolled condition. At acidic pH, MOC surface was highly protonated and more was electrostatic attraction between oxyanion of chromium and MOC. At uncontrolled pH condition, maximum 82% removal of total chromium was achieved at initial pH of 2. Removal of Cr(VI) was little higher of 90% (Fig. 5(a)). Final solution pH (uncontrolled pH condition) after Cr(VI) adsorption is given in Fig. 5(b). Proton was generated in pH range of 2 to 5 (pH increased to 2.3 and 5.3). At controlled pH of 2, maximum 60% removal of total chromium and 82% removal of Cr(VI) were achieved (Fig. 5(c)). Residual concentrations of Cr(III) as (%) of initial Cr(VI) are shown at uncontrolled and controlled pH in Fig. 5(b) and 5(d), respectively. Residual Cr(III) (%) was higher at controlled pH condition (3.6-23%) as compared to uncontrolled one (0.2-8%) and residual Cr(III) (%) decreased with increase in pH for both conditions. This results show that controlled pH condition favoured higher reduction of Cr(VI) to Cr(III) and this reduced Cr(III) remained in solution resulting lower removal of total chromium.

Removal of Hg(II) was studied by MOC from initial Hg(II) concentration of 50 mg/L with MOC dose of 2 g/L at uncontrolled condition. Initial solution of pH was adjusted at desired value (2 to 7). Under uncontrolled pH condition, at initial pH of 2, removal of Hg(II) was nearly negligible (8.5%) (Fig. 6). Hg(II) removal increased with increase in pH and maximum 90% removal was achieved at pH of 6. One control study was carried out without adsorbent to study the effect of pH on Hg(II) precipitation and it was observed that Hg(II) precipitation occurred at pH 6 and above. Since pH change occurred in uncontrolled condition (increase in pH at

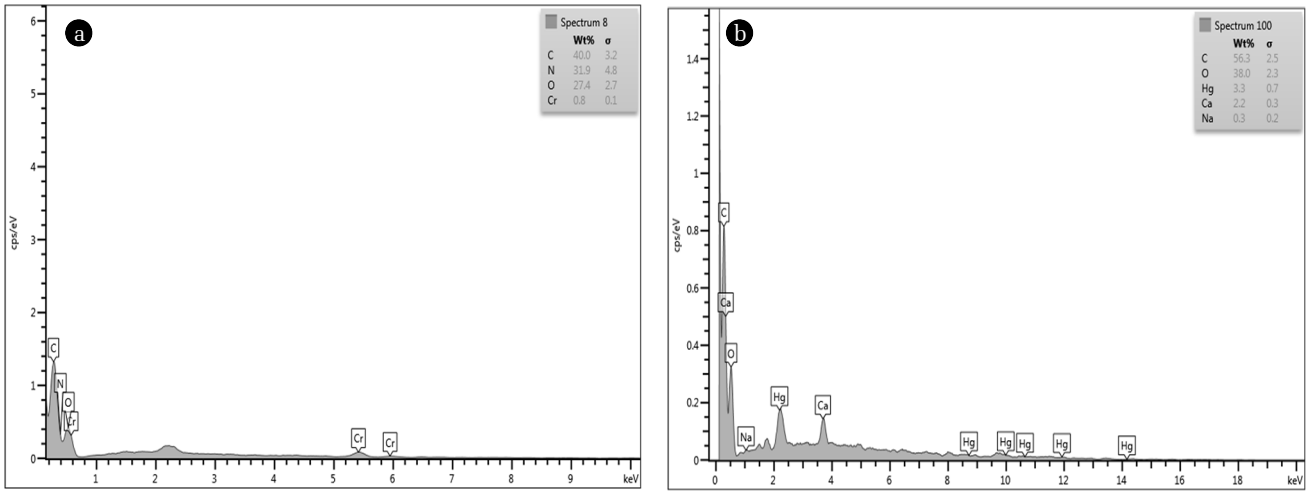

Fig. 4. EDX spectra of MOC after adsorption of (a) Cr(VI) and (b) Hg(II).

2-4 and drop in pH from 5 to 7), acetate buffer was used to control solution pH. Fig. 6 shows that maximum removal of 85% was achieved at pH of 5 at controlled pH and remained constant beyond that. It can be seen that both uncontrolled and controlled pH similar removal was obtained upto pH 5. From pH 6 and above, higher Hg(II) removal was achieved at uncontrolled pH condition, which could be due to precipitation. Further studies were conducted at uncontrolled pH with Cr(VI) and at controlled pH with Hg(II).

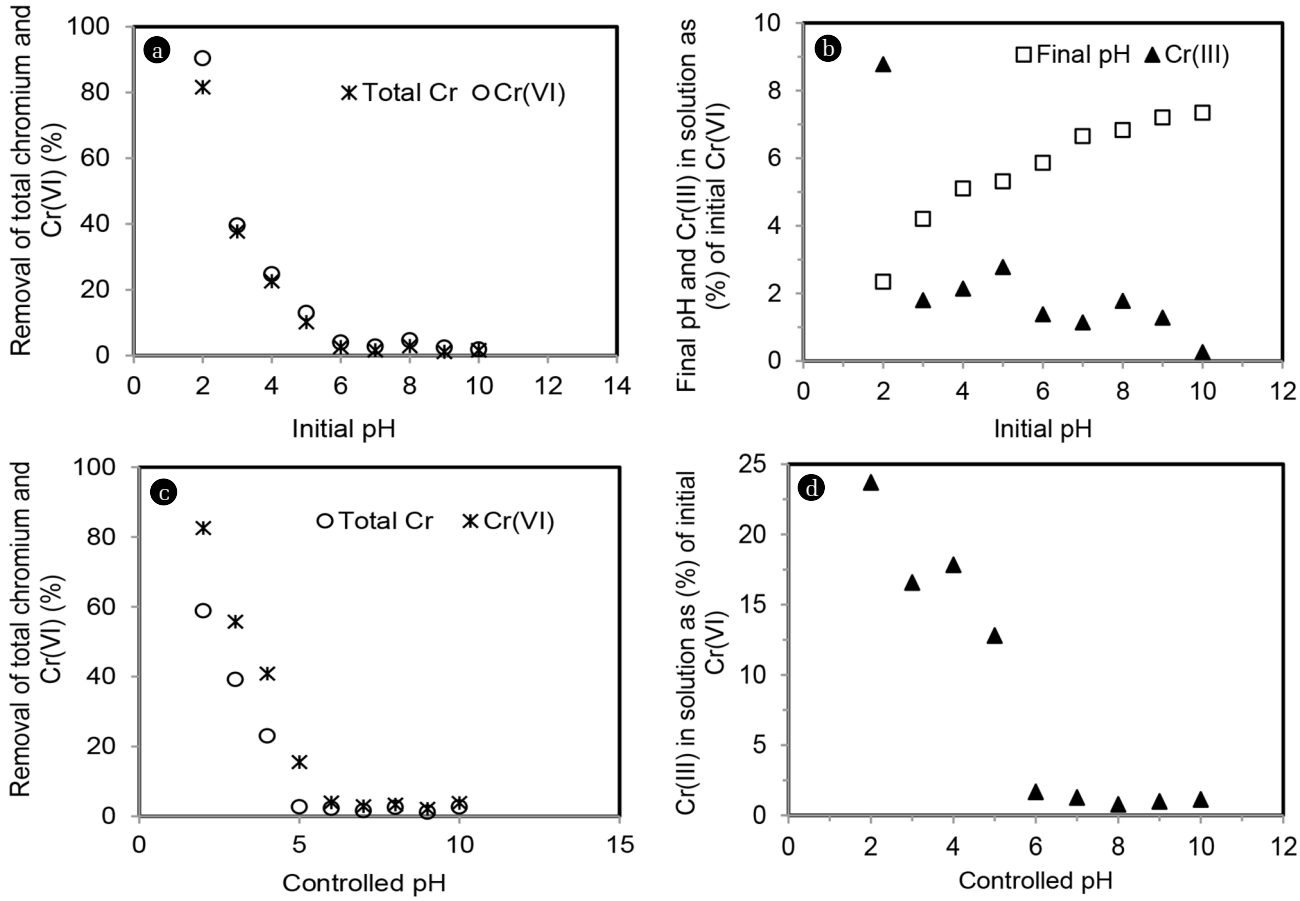

Fig. 5. (a) removals of total chromium and Cr(VI) at uncontrolled pH; (b) final pH and residual Cr(III) (%) at uncontrolled pH (c) removals of total chromium and Cr(VI) at controlled pH and (d) residual Cr(III) (%) at controlled pH.

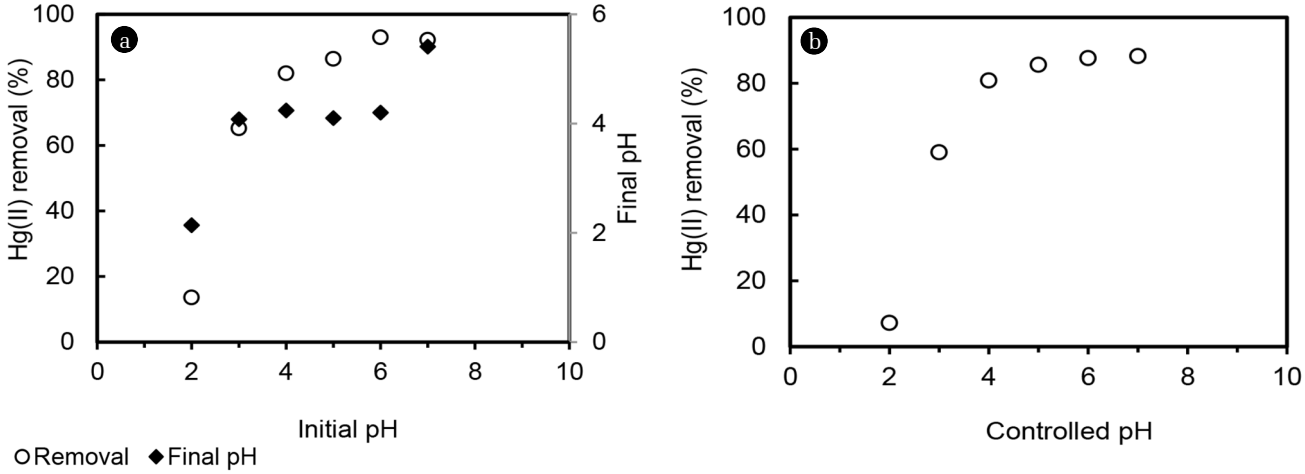

Fig. 6. Effect of solution pH on removal of Hg(II) at (a) uncontrolled pH and (b) controlled pH.

3.3. Effect of Adsorbent Dose

Effect of MOC dose on metal removal was studied varying adsorbent dose from 0.1 to 15 g/L. Dose variation study was carried out at two pH levels: 2 and 3 for Cr(VI) (uncontrolled) and 4 and 5 for Hg(II) (controlled) for 24 h. Equilibrium uptakes (q_e) of total chromium and Hg(II) are shown in Fig. 7. Maximum uptake of total chromium was 29 mg/g at pH of 2 and 23 mg/g at pH of 3. For Hg(II), maximum uptake achieved was 46 mg/g at pH 4 and 48 mg/g at pH 5. Uptake decreased with increase in MOC dose for both the metals due to unsaturation of adsorbent at a constant concentration of metal ion. Maximum Cr(VI) uptakes of 54.9 mg/g by waste plant biomass and 42.6 mg/g by brown seaweed were reported [14, 15]. Saman et al [16] reported Hg(II) adsorption capacity of 58 mg/g by rasped pith sago residue. Cork stoppers made from outer bark of oak tree was used for Hg(II) removal with an uptake of 18.7 mg/g [17].

3.4. Adsorption Isotherm

Several isotherm models like Langmuir, Freundlich, BET are available in literature to describe isotherm behavior and these models are given respectively in Eq. (3)-(5) [18].

$$q_e = \frac{Q_m\, b\, C_e}{1 + b\, C_e} \tag{3}$$

$$q_e = k_f\, C_e^{1/n} \tag{4}$$

$$q_e = \frac{Q_m\, B\, C_e}{(C_s - C_e)\left[1 + (B-1)\left(\frac{C_e}{C_s}\right)\right]} \tag{5}$$

where, Q_m is the adsorption capacity of the adsorbent (mg/g), b is the affinity constant for adsorption (L/mg) in Langmuir model (Eq. (3)). K_f is the Freundlich capacity factor and n is the index of heterogeneity (Eq. (4)). In BET model, Q_m is the amount adsorbed in a complete monolayer, B is equilibrium constant and C_s is the saturation concentration of adsorbate in water (Eq. (5)). The fitness of the isotherm model with experimental data was verified from correlation coefficient (R^2) and root mean square error (RMSE) (Eq. (6)).

$$RMSE = \sqrt{\frac{\sum_{i=1}^{n} (q_e - q_{ecal})^2}{n}} \tag{6}$$

where, q_e and q_{ecal} are metal uptakes observed experimentally and calculated using isotherm model, respectively and n is number of data points.

Isotherm plot for total chromium adsorption on MOC is shown in Fig. 8. Isotherm shape was concave type without any plateau both at pH 2 and 3 for total chromium. Based on isotherm classification scheme of Giles et al [19] and IUPAC [20], total chromium adsorption on MOC was of S1 and Type III at both pH 2 and 3. Langmuir model is suitable to predict convex type of isotherm and it failed to describe total chromium adsorption behavior. Nonlinear regression was carried out (MS Office, excel, Solver) to select the isotherm parameters for total chromium adsorption on MOC. It can be seen from Fig. 8 that BET model showed better correlation than Freundlich model at pH of 2 and at pH of 3, both BET and Freundlich models followed experimental data. Table 1 presents isotherm parameters. Based on higher R^2 and lower RMSE values, it can be decided that total chromium adsorption on MOC followed BET isotherm model at pH 2 and 3. S type isotherm for total chromium adsorption suggests low affinity between adsorbate and adsorbent at initial condition and increased affinity at higher equilibrium concentration of adsorbate. In this case the activation energy to remove adsorbate form aqueous phase was concentration dependent and adsorption was of cooperative type.

Hg(II) adsorption isotherm on MOC at pH of 4 and 5 are shown in Fig. 9. Both at pH 4 and 5, isotherm was convex type with a plateau and then both graphs showed upward curvature at higher

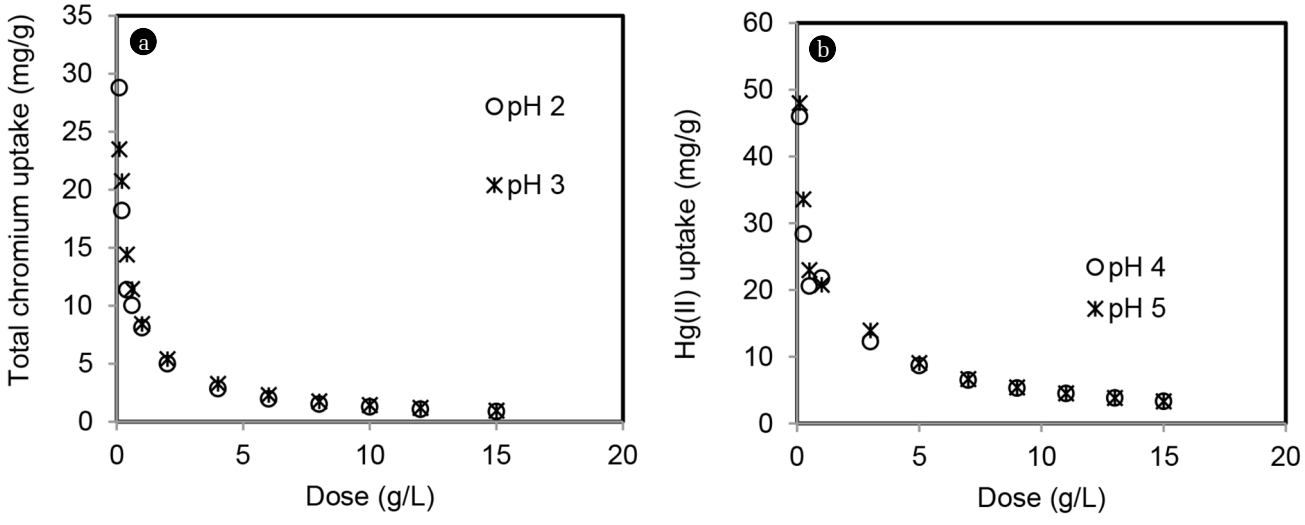

Fig. 7. Effect of MOC dose on uptakes of total chromium and Hg(II).

Table 1. Estimated Isotherm Parameters for Adsorption of Total Chromium on MOC

Isotherm model	Parameters	pH 2	pH 3
Freundlich	K_f	0.48	0.67
	n	0.71	0.71
	R^2	0.93	0.99
	RMSE	3.84	1.14
BET	Q_m (mg/g)	399.88	423.20
	C_s (mg/L)	18.94	47.35
	B (L/mg)	0.013	0.12
	R^2	0.97	0.99
	RMSE	1.83	0.95

equilibrium Hg(II) concentration (C_e > 40 mg/L). According to Giles classification this was of L3 type isotherm and based on IUPAC classification this was of Type II isotherm [19, 20]. This suggests unrestricted monolayer formation followed by multilayer formation. Both at pH of 4 and 5, monolayer formation was complete at C_e value of 38.5 mg/L with uptake 23 mg/g. Langmuir, Freundlich, BET isotherm were unable to describe this adsorption behavior of Hg(II) on MOC. A combined Freundlich-BET equation and a combined Langmuir-BET equation were tried (Eq. (7) and Eq. (8), respectively) [21].

$$q_e = k_f C_e^{\frac{1}{n}} + \frac{Q_m B C_e}{(C_s - C_e)\left[1+(B-1)\left(\frac{C_e}{C_s}\right)\right]} \quad (7)$$

$$q_e = \frac{Q_m b C_e}{1+bC_e} + \frac{Q_m B C_e}{(C_s - C_e)\left[1+(B-1)\left(\frac{C_e}{C_s}\right)\right]} \quad (8)$$

The plot of isotherm data with fitted models for Hg(II) is shown in Fig. 9. In Table 2, model parameters with R^2 and RMSE values are given. It can be seen that both the models fitted Hg(II) adsorption

Table 2. Estimated Isotherm Parameters for Adsorption of Hg(II) on MOC

Isotherm model	Parameters	pH 4	pH 5
BET-Freundlich	Q_m (mg/g)	339	341
	K_{BET}	0.0005	0.0018
	C_s (mg/L)	49.60	52.58
	K_f	3.67	5.83
	n	1.95	3.02
	R^2	0.98	0.98
	RMSE	2.16	1.54
BET-Langmuir	Q_m (mg/g)	24.98	18.79
	K_{BET}	0.0011	0.054
	C_s (mg/L)	43.68	52.94
	B	0.14	0.25
	R^2	0.99	0.98
	RMSE	1.85	2.11

data with R^2 of 0.98-0.99. At pH of 4, BET-Langmuir model was the most appropriate while at pH 5, BET-Freundlich model was ideal.

This monolayer followed by multilayer formation was due to blockage of pores of MOC. Isotherm study was carried out at a fixed concentration of Hg(II) with varying dose of MOC. When MOC dose was very high (more sites as compared to metal ion), Hg(II) ion did not penetrate through the pores of MOC. Instead, Hg(II) was adsorbed by functional groups at the outer layer of inners surface of MOC. This adsorbed Hg(II) ion formed a cluster near outer layer of MOC and blocked the pores of MOC and metal ions could not diffuse to functional groups present within the interior surface on MOC due to pore blockage. When MOC dose was less (at same initial Hg(II) concentration), the Hg(II) penetrated deep inside the pores until pores were completely occupied. Similar pore blockage was reported during adsorptions of Cd(II) by porous magnetic chitosan beads [22] and phenol by macroreticular resin [21].

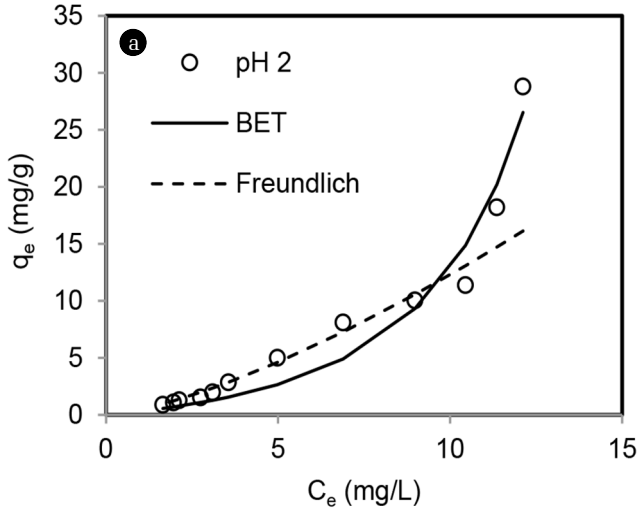

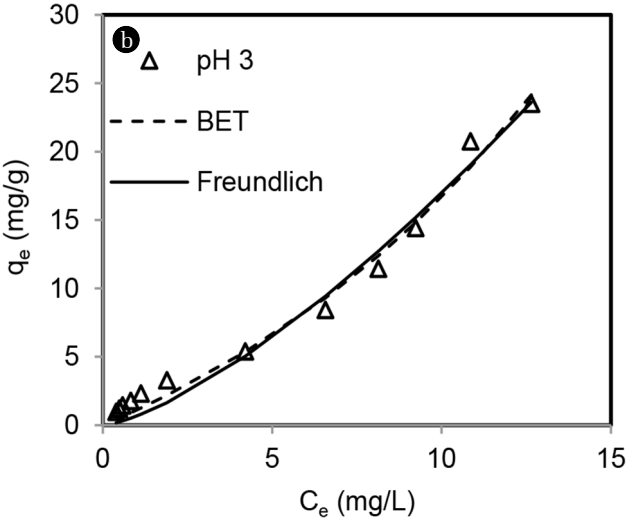

Fig. 8. Isotherm plots of total chromium on MOC at pH 2 and 3.

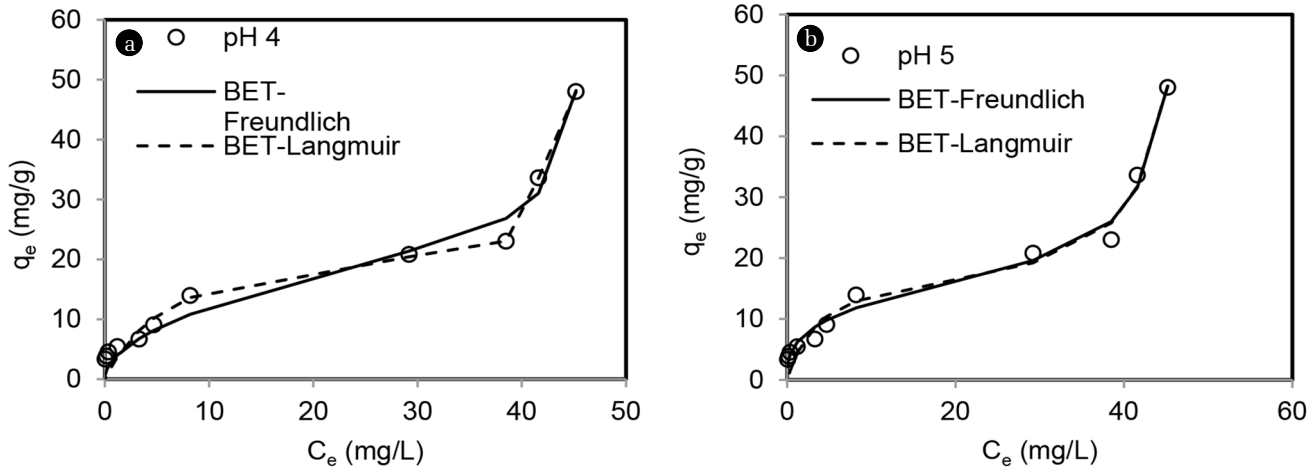

Fig. 9. Isotherm plots of Hg(II) on MOC at pH (a) 4 and (b) 5.

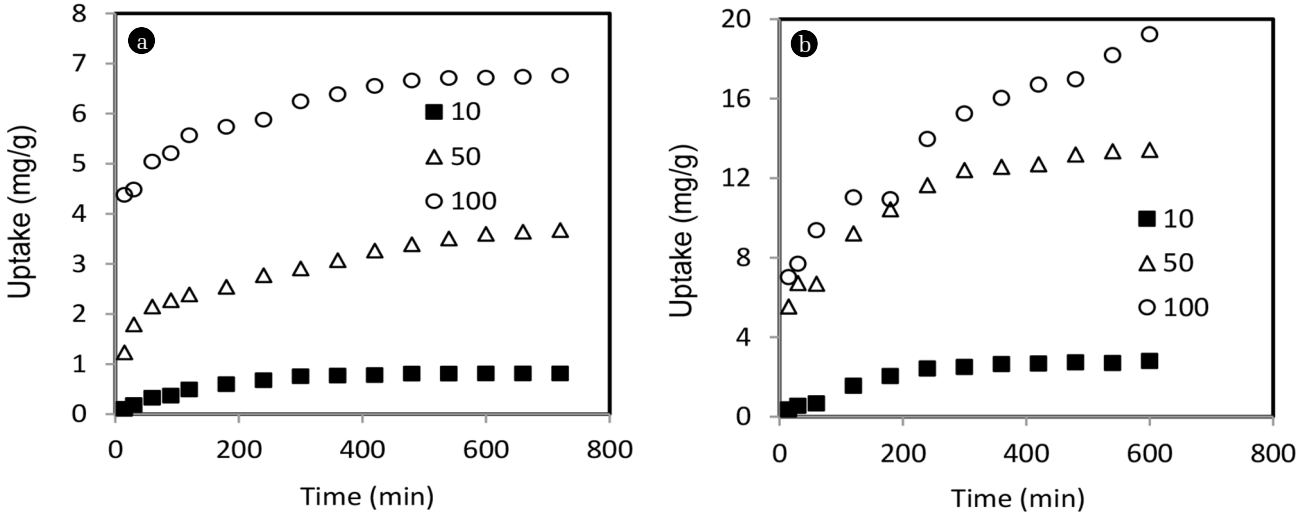

Fig. 10. Adsorption kinetics of (a) total chromium and (b) Hg(II) on MOC.

3.5. Effect of Initial Metal Ion Concentration

Uptakes of total chromium and Hg(II) at varying initial concentrations of 10, 50 and 100 mg/L are shown in Fig. 10. For Cr(VI), initial pH was 3 and solution pH was left uncontrolled. For Hg(II) study was carried out at constant pH of 4. For both the metals, uptake and equilibrium time increased with increase in initial concentrations. The initial concentration provides an important driving force to overcome mass transfer resistance of the adsorbate and adsorbent surface and uptake of metal ion increased.

3.6. Adsorption Kinetics

In order to find out the governing step of adsorption process, kinetic data of total chromium and Hg(II) on MOC were analyzed using intraparticle diffusion model [23] (Eq. (9)).

$$q_t = k_i t^{0.5} + y \quad (9)$$

where k_i is the rate of intraparticle diffusion (mg/L.min$^{0.5}$). Intercept, y gives the information on the thickness of the boundary layer and if intercept is zero, then intraparticle diffusion is the sole rate limiting step in adsorption. Plots of q_t vs. $t^{0.5}$ are shown in Fig. 11. For Cr(VI), none of the plots passed through origin and three linear regions were observed. The initial sharper portion suggests external surface adsorption followed by gradual adsorption due to intraparticle diffusion and the third region suggests equilibrium stage. For Hg(II), at initial concentration of 10 and 50 mg/L, two linear regions were observed with initial film diffusion followed by intraparticle diffusion. When initial Hg(II) was 100 mg/L, single line was obtained, but it did not pass through origin. This result suggests that intraparticle diffusion was involved but not the sole rate limiting step in adsorptions of total chromioum and Hg(II) by MOC. The rate constant of intraparticle diffusion (k_i) was determined from the slope of the intraparticle diffusion line (second region of q_t vs $t^{0.5}$ plot) and values of k_i are given in Table 3. The values of k_i increased with increasing initial Cr(VI)and Hg(II) concentrations. The increase in initial metal con-

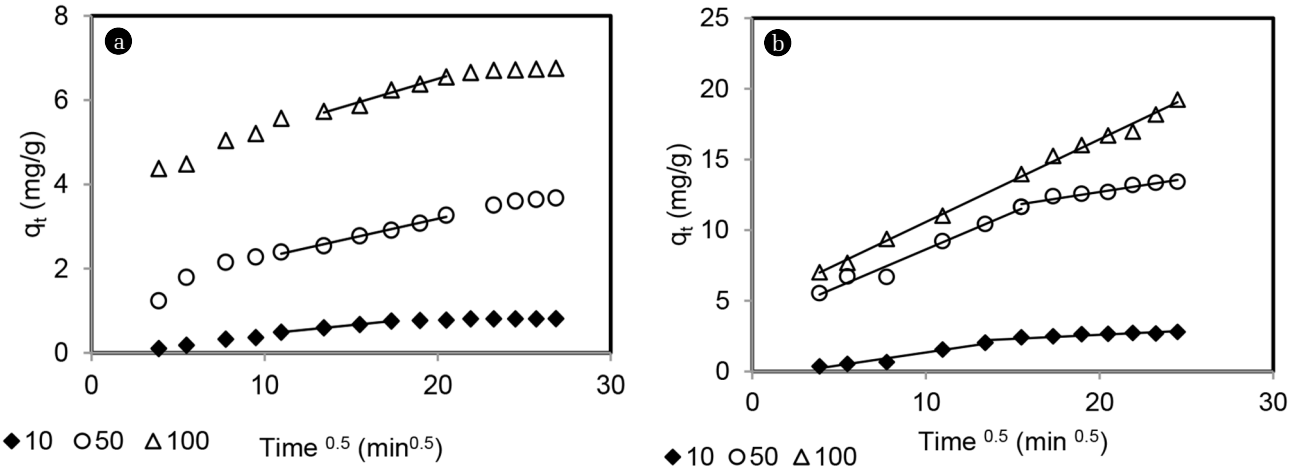

Fig. 11. Intraparticle diffusion plots for (a) total chromium and (b) Hg(II) on MOC.

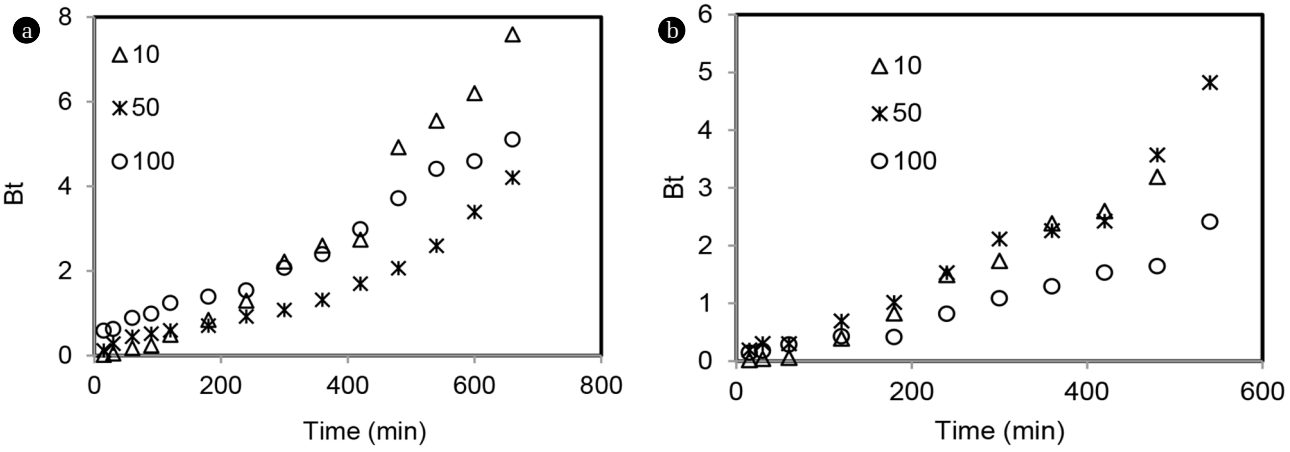

Fig. 12. Boyd's plots for (a) total chromium and (b) Hg(II) on MOC.

centration results in an increase of the driving force of adsorption, which caused higher intraparticle diffusion rate.

A model proposed by Riechenberg [24] (Eq. (10)) was also used to further confirm the role of external mass transfer during removals of Cr(VI) and Hg(II) by MOC.

$$F = 1 - \frac{6}{\pi^2} \Sigma_{n=1}^{\infty} \frac{1}{n^2} \exp\left(\frac{-n^2 D_s \pi^2 t}{R^2}\right) \quad (10)$$

where, $F = \frac{q_t}{q_e}$, t is time (min), q_t and q_e are metal uptakes at time t and equilibrium, respectively, D_s is the effective diffusion coefficient of adsorbate in adsorbent phase (cm^2/min), n is an integer that defines the infinite series solution and R is radius of adsorbent particle. Eq. (10) is modified by substituting B for $\frac{\pi^2 D_s}{r^2}$ in Eq. (11).

$$F = 1 - \frac{6}{\pi^2} \Sigma_{n=1}^{\infty} \frac{1}{n^2} \exp(n^2 Bt) \quad (11)$$

Reichenberg provided table for Bt value for each value of F, which was used to determine Bt values at any time t, corresponding to that F (fractional uptake). Bt vs. time were plotted (Boyd's plot) and shown in Fig. 12. If Boyd's plot is linear and passes through origin, it suggests that adsorption is governed by particle diffusion, otherwise it is controlled by film diffusion [22]. The plots were nonlinear and did not pass through origin for both total chromium and Hg(II), suggesting film diffusion controlled the adsorption process for the studied concentration range (10-100 mg/L).

For each initial Cr(VI) and Hg(II) concentration, the slope of the line (i.e. B) was determined from the linear portion of Bt vs. time plots and given in Table 3. From B values, effective diffusion coefficients (D_s) were calculated ($B = \frac{\pi^2 D_s}{R^2}$). Radius (R) of MOC particle was considered as 328 μm (mean diameter of 657 μm from particle size analysis). Effective diffusion coefficient (D_s) values are given in Table 3. For Cr(VI), diffusion coefficient was independent of initial metal ion concentration and for Hg(II) it

Table 3. Kinetic Parameters of Total Chromium and Hg(II) Adsorption on MOC

Initial metal concentration (mg/L)	Intraparticle diffusion model			Reichenberg's model	
	R^2	k_i (mg/g. $min^{0.5}$)	Intercept	B (/min)	Ds (m^2/sec)
		Cr(VI)			
10	0.99	0.041	0.041	0.007	1.2×10^{-16}
50	0.95	0.091	1.35	0.004	0.7×10^{-16}
100	0.98	0.121	4.07	0.007	1.2×10^{-16}
		Hg(II)			
10	0.97	0.058	1.42	0.007	1.2×10^{-16}
50	0.99	0.248	7.63	0.006	1×10^{-16}
100	0.99	0.584	4.73	0.003	0.5×10^{-16}

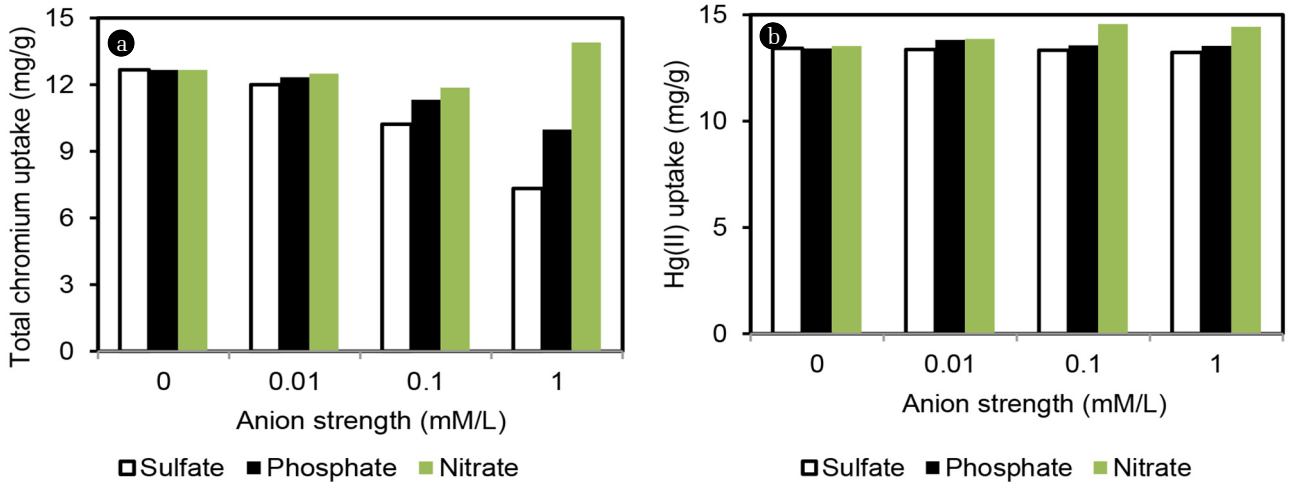

Fig. 13. Effects of other ions on uptake of total chromium and Hg(II) by MOC.

decreased with increase in initial Hg(II) concentration. For Cr(VI) and Hg(II), average D_s values calculated were 6.54×10^{-11} cm^2/min (1.09×10^{-16} m^2/sec) and 5.82×10^{-11} cm^2/min (0.97×10^{-16} m^2/sec), respectively. These indicate that metal adsorption by MOC in the studied range was governed by external mass transfer, diffusion also occurred very slowly through MOC pores.

3.7. Effect of Other Ions on Metal Ion Adsorption

The effects of other anions on total chromium and Hg(II) adsorptions on MOC is shown in Fig. 13. Three anions named phosphate, sulfate and nitrate of varying strength (0.01-1 mM/L) was used along with a control (without anion). None of the three anion showed any inhibitory effect on Hg(II) uptake. For total chromium adsorption, inhibition was in the order of sulfate > phosphate > nitrate. Total chromium removal decreased by almost 50% due to competitive effect of sulfate anion. Cr(VI) remains in solution in the form of oxyanion [$HCrO_4^-$] and anions like like SO_4^{2-} and HPO_4^{2-}, inhibited adsorption of $HCrO_4^-$ on MOC. Hg(II) remains in solution either as $HgCl_2$, or Hg(II) and its adsorption was independent of other anions in solution.

3.8. Desorption and Reuse

Desorption of total chromium was studied using NaOH and results are shown in Fig. 12(a). Maximum 25% desorption was achieved with 2 N NaOH and beyond this strength, desorption decreased. It was observed that more than 90% of desorbed chromium was in the form of Cr(VI) (Fig. 14(a)). In order to recover Cr(III), a chelating agent like EDTA was used and only 10% desorption was achieved at EDTA strength of 1 N (data not shown). Poor desorption of total chromium could be due to conversion of Cr(VI) to Cr(III) either before /after adsorption process on MOC.

Desorption of Hg(II) from MOC was performed using different strengths (0.5-5 N) of HCl, NaOH and KI and results are shown in Fig. 14(b). NaOH and KI showed higher desorption of Hg(II) than HCl. With NaOH, maximum desorption was around 70% at 3 N NaOH. When desorption was carried out using KI, maximum desorption of 60% was obtained at 1 N strength of KI. With HCl, maximum 32% desorption was achieved when strength was 5 N. Hg(II) makes strong complexes with iodine present in KI and caused desorption.

After desorption with NaOH, reuse of MOC was studied in four cycles and results are shown in Fig. 14(c). With each cycle, uptakes of metals decreased. Total chromium uptake decreased by 33% and 77% from 1^{st} to 2^{nd} and 1^{st} to 4^{th} cycle. Corresponding decrease with Hg(II) was 28% and 93%, respectively.

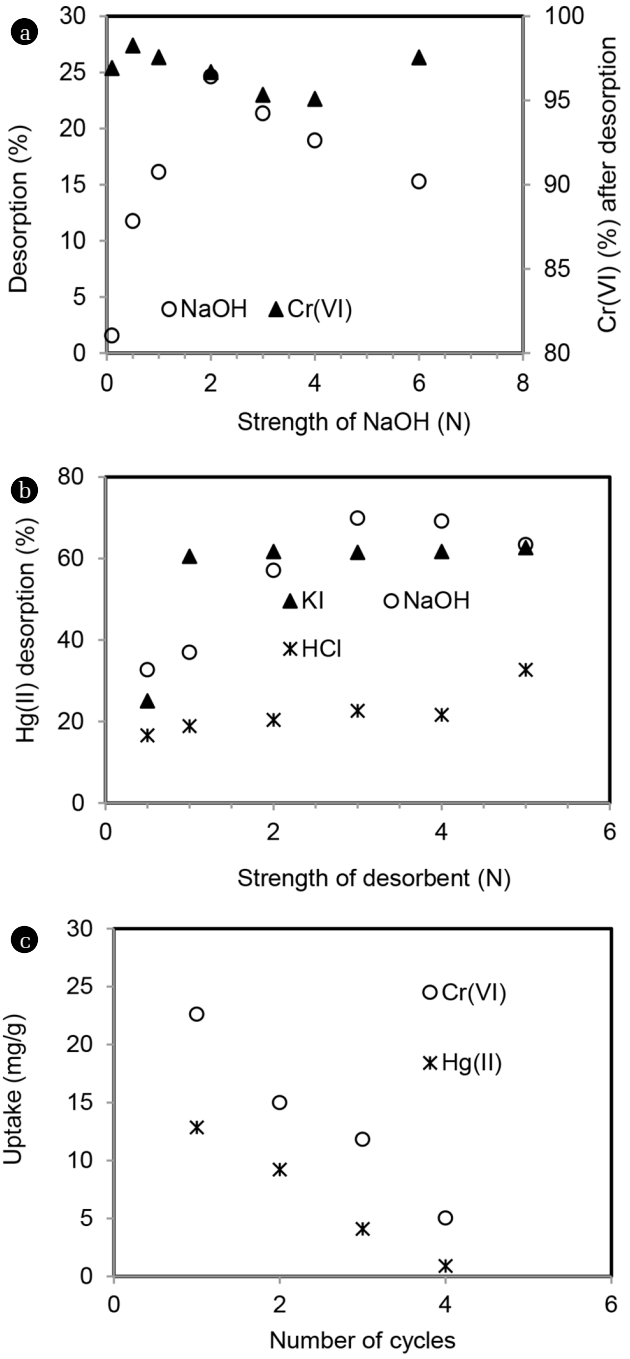

Fig. 14. (a) desorption of chromium (b) desorption of Hg(II) and (c) reuse of chromium and Hg(II) from MOC.

3.9. Metal Removal Mechanism by MOC

Cr(VI) remains in solution as oxyanions like $HCrO_4^-$ and $Cr_2O_7^{2-}$ ion (from pH 2-6), and CrO_4^{2-} (above pH 6) [4]. Adsorption of Cr(VI) form solution can take place either by ion exchange mechanisms of oxyanion [$HCrO_4^-$ and $Cr_2O_7^{2-}$], or chemical reduction to Cr(III) and complexation of Cr(III) or by a combination of both mechanism.

Zero point charge of MOC was also observed at 5.3 and below this pH, adsorbent surface was protonated. FTIR study showed that MOC surface had amine ($-NH_2$) and carboxylic (R-COOH) groups. pH study showed that acidic pH favoured total chromium adsorption (section 3.2). At acidic pH, amine was in protonated form ($-NH_3^+$) and it adsorbed oxyanion $HCrO_4^-$ by ion exchange mechanism.

Some reduction of Cr(VI) also occurred during adsorption by MOC (Fig. 5(b) and 5(d)) and reduction was more in controlled pH condition. Literature reports mentioned that carboxylic group and lignin groups present on MOC surface can behaved as electron donor [25]. The reduction reaction of Cr(VI) is given in Eq. (12) and it shows that more the availability of H+, higher will be forward reaction i.e. more Cr(III) formation.

$$HCrO_4^- + 7H^+ + 3e^- \rightarrow Cr^{3+} + 4H_2O \quad (12)$$

In controlled pH condition more proton was available (in the form of acetate buffer, to prevent pH increase) and more proton favoured higher reduction of Cr(VI) than uncontrolled pH. Cr(III) remains in aqueous solution as Cr^{3+} (dominant specie from pH 1-3), $Cr(OH)_2^+$(available form pH 3, equimolar with Cr^{3+} at pH 4 and dominant at pH 5) and $Cr(OH)_2^+$ (available pH $\geq$ 5) [26]. At low pH (below pHzpc), MOC surface was protonated and no adsorption of Cr(III) species occurred due to charge repulsion and higher Cr(III) was observed in solution at acidic pH. Above pHzpc, MOC surface was in deprotonated form and Cr(III) species can form complexation with amine and carboxyl groups of deprotonated MOC. It can be concluded that both at uncontrolled and controlled pH condition at pH of 2-4, total chromium removal occurred by ion exchange mechanism. In presence of other anions, total chromium removal decreased significantly (section 3.7). Previous researchers mentioned that when Cr(VI) removal was strongly inhibited by presence of anions in solution, ion exchange was responsible mechanism for Cr(VI) uptake, otherwise chemical reduction was responsible mechanism [27]. At pH 5, surface protonation of MOC was very less and ion exchange was negligible and small amount of total chromium removal was achieved (2-10%), which could be due to complexation of Cr(III) and deprotonated MOC. However, after adsorption of Cr(VI) by ion exchange mechanism, some fraction of this adsorbed Cr(VI) could be reduced by several functional groups on MOC surface. Since Cr(III) is kinetically almost immobile [with lignad exchange rate of 2×10^{-6}/s of water molecule from the first coordination sphere of Cr(III)] [28], this reduced Cr(III) remained on the MOC surface. In desorption study, only 25% of chromium was released to solution by NaOH and the remaining 75% was in the form of Cr(III) and remained on MOC surface.

In aqueous solution Hg(II) makes soluble complexes with both OH^-, Cl^- ions like $HgCl^+$, $HgCl_{2(aq)}$, $HgCl_3^-{}_{(aq)}$, $HgClOH_{(aq)}$ and $HgCl_4^{2-}{}_{(aq)}$. In this study source of Hg(II) was $HgCl_2$ salt. The very high value of formation constant of $HgCl_2$ of $10^{13.23}$ suggests that $HgCl_2$ does not dissociate/ionize in aqueous solution to form $HgCl^+{}_{(aq)}$, $Hg^{2+}{}_{(aq)}$, $HgClOH_{(aq)}$ [29] and it can be considered that $HgCl_{2(aq)}$ remained only available specie in solution. Anionic species like $HgCl^-{}_{3(aq)}$ and $HgCl^{2-}{}_{4(aq)}$ are available only when Cl^- ion in

solution is very high and can be ruled out in this study.

In the present study with MOC, acetate buffer was used to control pH and Hg(II) can form soluble complexes like $HgCH_3COO^+_{(aq)}$, $HgCH_3COO_{(aq)}$. During pH study it was observed that Hg(II) removal remained almost same in uncontrolled pH (absence of acetate) and controlled pH (presence of acetate ion) upto pH of 5, suggesting no remarkable affect of acetate on Hg(II) adsorption from $HgCl_2$. In pH study (Fig. 6) Hg(II) removal increased with increasing pH. With increase in pH both amine and carboxylic group was in deprotonated forms of $-NH_2$ and $R-COO^-$, respectively and can form complex with $HgCl_2$ [30]. At acidic pH, these functional groups on MOC was more protonated ($-NH_3$) and (R-COOH) forms and formed weaker interaction with $HgCl_2$ so removal of Hg(II) decreased. Since complexation was main mechanism for $HgCl_2$ uptake, it was independent of presence of anions in solution. During desorption with HCl, release of Hg(II) ion in solution was lesser than NaOH, which could be due to formation of anionic species $HgCl^-_{3(aq)}$ and $HgCl^{2-}_{4(aq)}$ and adsorption of these by protonated MOC.

4. Conclusions

Adsorption behavior of hexavalent chromium [Cr(VI)] and mercury ($HgCl_2$) on MOC was studied by analyzing adsorption isotherm and kinetics. Characterization studies showed that the mean particle size of MOC was 657 μm and presence of amine and carboxylic groups on MOC surface and pore size distribution of 5-20 nm. The optimum pH for total chromium adsorption was observed in acidic range (2-3) and Hg(II) was from 4-5. Maximum adsorption capacities of total chromium and Hg(II) were observed as 29 mg/g and 48 mg/g, respectively. Total chromium adsorption isotherm was of S1 type and concave shape with cooperative adsorption and followed BET isotherm model. Hg(II) isotherm was of L3 type with initial monolayer followed by multilayer formation. A combined BET-Langmuir was observed as appropriate for Hg(II) adsorption at pH 4 and a combined BET-Freundlich model was ideal for pH 5. Blockage of pores of MOC caused lesser uptake of Hg(II) at lower concentration. Kinetics studies showed that both total chromium and Hg(II) adsorption was governed by external mass transfer. Ion exchange was dominant mechanism for total chromium adsorption and reduction occurred on MOC surface by functional groups. Reduced Cr(III), being highly immobile, desorption was very less. Hg(II) was removed as $HgCl_2$ by deprotonated amine/carboxylic groups of MOC.

References

1. Zhou J, Wang Y, Wang J, Qia W, Long D, Ling L. Effective removal of hexavalent chromium from aqueous solutions by adsorption on mesoporous carbon microspheres. *J. Colloid Interf. Sci.* 2016;462:200-207.
2. Liu T, Wang Z, Yan X, Zhang B. Removal of mercury(II) and chromium(VI) from wastewater using a new and effective composite: Pumice-supported nanoscale zero-valent iron. *Chem. Eng. J.* 2014;245:34-40.
3. Central Pollution Control Board. General standards for discharge of environmental pollutants part-A: Effluents. Schedule VI of Environment (protection) third amendment rules, India; 1993.
4. Dinker MK, Kulkarni PS. Recent advances in silica-based materials for the removal of hexavalent chromium: A review. *J. Chem. Eng. Data* 2015;60:2521-2540.
5. Feng N, Guo X, Liang S, Zhu Y, Liu J. Biosorption of heavy metals from aqueous solutions by chemically modified orange peel. *J. Hazard. Mater.* 2011;185:49-54.
6. Gupta VK, Nayak A, Agarwal S. Bioadsorbents for remediation of heavy metals: Current status and their future prospects. *Environ. Eng. Res.* 2015;20:1-18.
7. Khan MA, Ngabura M, Choong TSY, Masood H, Chuah LA. Biosorption and desorption of Nickel on oil cake: Batch and column studies. *Bioresource Technol.* 2012;103:35-42.
8. Bulgariu L, Hlihor RM, Bulgariu D, Gavrilescu M. Sorptive removal of cadmium(II) ions from aqueous solution by mustard biomass. *Environ. Eng. Manage. J.* 2012;11:1969-1976.
9. Ajmal M, Rao RAK, Khan MA. Adsorption of copper from aqueous solution on *Brassica cumpestris* (mustard oil cake). *J. Hazard. Mater.* 2005;B122:177-183.
10. Fiol N, Villaescusa E. Determination of sorbent point zero charge: Usefulness in sorption studies. *Environ. Chem. Lett.* 2009;7:79-84.
11. APHA, AWWA, WPCF. Standard methods for the examination of water and wastewater. 21st ed. Washington D.C.: American Public Health Association; 2005.
12. Saha B, Chakraborty S, Das G. Trimesic acid coated alumina: An efficient multi-cyclic adsorbent for toxic Cu(II). *J. colloid Interf. Sci.* 2008;320:30-39.
13. Kalsi PS. Spectroscopy of organic compounds. 6th ed. Delhi: New Age International Publishers; 1994. p. 108-110.
14. Mishra A, Dubey A, Shinghal S. Biosorption of chromium(VI) from aqueous solutions using waste plant biomass. *Int. J. Environ. Sci. Technol.* 2015;12:1415-1426.
15. Bertagnolli C, Silva MGC, Guibal E. Chromium biosorption using the residue of alginate extraction from *Sargassum filipendula*. *Chem. Eng. J.* 2014;237:362-371.
16. Saman N, Johari K, Tien SS, Mat H. Removal of Hg(II) and $CH_3Hg(I)$ using rasped pith sago residue biosorbent. *Clean-Soil Air Water* 2014;42:1541-1548.
17. Lopes CB, Oliveira JR, Rocha LS, et al. Cork stoppers as an effective sorbent for water treatment: the removal of mercury at environmentally relevant concentrations and conditions. *Environ. Sci. Pollut. Res.* 2014;21:2108-2121.
18. Foo KY, Hameed BH. Insights into the modeling of adsorption isotherm systems. *Chem. Eng. J.* 2010;156:2-10.
19. Giles CH, Smith D, Huitson A. A general treatment and classification of the solute adsorption isotherm. I: Theoretical. *J. Colloid Interf. Sci.* 1974;47:755-765.
20. Sing KSW, Everett DH, Haul RAW, et al. Reporting physisorption data for gas/solid systems with special reference to the determination of surface area and porosity. *Pure Appl. Chem.* 1985;57:603-619.
21. Juang R, Shiau J. Adsorption isotherms of phenols from water onto macro reticular resins. *J. Hazard. Mater.* 1999;B70:171-183.

22. Rorrer GL, Hsien T. Synthesis of porous-magnetic chitosan beads for removal of cadmium ions from waste water. *Ind. Eng. Chem. Res.* 1993;32:2170-2178.
23. Weber WJ, Morris JC. Kinetics of adsorption on carbon from solutions. *J. Sanit. Eng. Div. Am. Soc. Civ. Eng.* 1963;89:31-60.
24. Reichenberg D. Properties of ion-exchange resins in relation to their structure. III. Kinetics of exchange. *J. Am. Chem. Soc.* 1953;75:589-597.
25. Krishnani KK, Meng X, Christodoulatos C, Boddu VM. Biosorption mechanism of nine different heavy metals onto biomatrix from rice husk. *J. Hazard. Mater.* 2008;153:1222-1234.
26. Kumar PA, Ray M, Chakraborty S. Adsorption behaviour of trivalent chromium on amine-based polymer aniline formaldehyde condensate. *Chem. Eng. J.* 2009;149:340-347.
27. Lee M, Hong K, Shin-Ya Y, Kajiuchi T. Adsorption of hexavalent chromium by chitosan-based polymeric surfactants. *J. Appl. Polymer Sci.* 2005;96:44-50.
28. Lippard SJ, Berg JM. Principles of bioinorganic chemistry. Mill Valley, CA: Univ. Science Books; 1994. p. 21-22, 28-29.
29. Kawamura Y, Mitsuhashi M, Tanibe H. Adsorption of metal ions on polyaminated highly porous chitosan chelating resin. *Ind. Eng. Chem. Res.* 1993;32:386-391.
30. Das SK, Das AR, Guha AK. A study on the adsorption mechanism of mercury on *Aspergillus versicolor* biomass. *Environ. Sci. Technol.* 2007;41:8281-8287.